Multiscale Image Contrast Amplification (MUSICA™)

Pieter Vuylsteke, Emile Schoeters

Agfa-Gevaert N.V. B-2640 Mortsel, Belgium

ABSTRACT

This article presents a novel approach to the problem of detail contrast enhancement, based on a multiresolution representation of the original image. The image is decomposed into a weighted sum of smooth, localised, two-dimensional basis functions at multiple scales. Each transform coefficient represents the amount of local detail at some specific scale and at a specific position in the image. Detail contrast is enhanced by non-linear amplification of the transform coefficients. An inverse transform is then applied to the modified coefficients. This yields a uniformly contrast-enhanced image without artefacts. The MUSICA-algorithm is being applied routinely to computed radiography images of chest, skull, spine, shoulder, pelvis, extremities, and abdomen examinations, with excellent acceptance. It is useful for a wide range of applications in the medical, graphical, and industrial area.

1. INTRODUCTION

Optimal contrast rendition is a critical issue in conventional radiology. X-ray screen-film systems have an S-shaped gradation curve with an exposure range of the order of 100:1. The range of linear response is even ten times as small. The exposure margins are small for most examinations: under- or overexposed images have zero contrast in the bright or dark areas respectively. The local slope of the gradation curve determines the minimum perceptible attenuation difference at a given exposure level. The shape of this curve is critical since it determines the distribution of contrast across the available dynamic range. If it is too generous in one part of the exposure range, it will be insufficient in some other subrange. Clearly accurate exposure control and appropriate choice of film gradation are essential requirements in conventional radiography.

In computed radiography (CR) the detector is a stimulable phosphor screen. The major difference of this technology with conventional X-ray imaging is the fact that the stored latent image can be retrieved by stimulating the phosphor locally with a light beam. The light emitted from the screen after stimulation is proportional to the amount of irradiation. The stimulable phosphor screen is read out in a separate reading apparatus consisting of a laser scanning device and a light sensor combined with a digitising device. A CR system accommodates to a much larger dynamic range than a screen-film system, nearly 1000:1 within a single image, so the problem of applying the correct exposure dose becomes less critical than in conventional radiography as far as the image capture is concerned. But the above-mentioned trade-off of image contrast against dynamic range reappears at the output stage, being film hard copy or CRT display screen, where the optical density range is limited to 2.5D or 1.5D respectively, under normal viewing conditions.

The dynamic range of the CR readout system is large enough to catch all the diagnostic information plus additional margin for under- or overexposure, certainly, but this whole range cannot be displayed with acceptable contrast. However, the dynamic range of the diagnostically relevant parts of the image is much smaller than the detected range. In systems without prescan the relevant diagnostic range is determined through analysis of the scanned data, and the selected subrange is remapped onto the entire range of the output medium. This function ensures that the average image brightness is within certain limits insensitive to exposure fluctuations. The gradation of the final image can be shaped with much more flexibility than in a screen-film system since it is defined in computational terms instead of being predetermined by the physico-chemical properties of a specific film emulsion. For this reason CR images can have optimised gradation for different examination types. If desired a single original image can generate two or more processed images with different gradation.

Although in a CR system the limited density range is used in a consistent and nearly optimal way, the intrinsic signal range may still be too large for proper viewing. In examinations such as shoulder, pelvis, and ankle, diagnostic features appear in a wide density range across the image. Optimising the image gradation only does not guarantee proper perception of subtle details everywhere: in dense bone structures, in weak tissue, or in dark weak tissue-bone interface regions, e.g. the border of a pelvic bone, contrast may be below the perceptual threshold.

0-8194-1462-X/94/$6.00

Most of the approaches for enhancing detail contrast are based on local neighbourhood operations. Adaptive histogram equalisation[1] and unsharp masking[2] are well-known techniques for this purpose. Adaptive histogram equalisation aims at stretching the contrast in smooth image regions. Unsharp masking tends to amplify the higher spatial frequency components in the image. The size of the operator kernel determines the spatial frequency band in which these enhancement techniques are active. For good performance the kernel size has to be tuned to the size of the details of interest. However, the most relevant sizes are not always known in advance. Adapting the kernel size to the specific radiological examination type may sometimes be feasible, but diagnostic details often occur at different scale levels within the same image (even within close vicinity), in which case the results remain unsatisfactory despite fine tuning attempts. The multiple experimental studies on optimal parameter tuning for unsharp masking confirm that this is a non-trivial problem[3,4]. The creation of artefacts in the vicinity of abrupt signal transitions, e.g. at bone-soft tissue boundaries, is an other common complaint of most contrast enhancement techniques based on sliding neighbourhoods. These artefacts have a detrimental effect on diagnosis; in some cases they suggest pathological evidence in a normal radiograph, in other cases they can hide subtle lesions[5,6]. Many improvements of the basic enhancement techniques specifically address the suppression of these artefacts[7,8].

This article presents a novel approach to the problem of detail contrast enhancement, operating on a multiresolution representation of the original image. The basic idea is to selectively amplify detail amplitude across the image plane, and across all resolution levels. Throughout this article the term "detail" indicates the local signal variations in the image. Detail is localised in spatial domain, it has a limited spatial extent, and it has a certain amplitude, which is essentially a differential value. Signal variations with a small spatial extent (high spatial frequency) are called "high resolution", "small scale", or "fine" details without any distinction; the widely extending signal variations (low frequency), are called "low resolution", "large scale", or "coarse" details. Low amplitude details are called "subtle"; these can either be fine or coarse.

2. THE MUSICA ALGORITHM

In the MUSICA-algorithm subtle details, i.e. image components having low detail *amplitude*, are amplified relative to the high amplitude details, at *all scales*. This is fundamentally different from the conventional approaches for detail contrast enhancement, which essentially stress a specific spatial frequency band. Our algorithm involves three basic steps:

1. Decomposing the original image into a multiresolution pyramid representing local detail at all scales.
2. Modifying the pyramid values according to a non-linear conversion function, which stresses the low amplitude values and reduces the large amplitudes.
3. Applying the inverse of the decomposition operator to the modified detail pyramid, to obtain a contrast enhanced image.

A first issue concerns the choice of *representation.* Any image can be expressed as a weighted sum of two-dimensional basis functions, by means of a linear transform. A few common examples are cited here for introducing some transform properties that are important in the current context: the Fourier transform (FT), the discrete cosine transform (DCT), and the Haar transform. The Fourier transform is perhaps the best known linear transform. The corresponding basis functions are orthonormal, periodic and extend across the whole image. In typical applications of the discrete cosine transform (DCT) such as image compression, it is common practice to partition the original image into non-overlapping blocks before applying the transform. In this case the basis functions are confined to image tiles of predetermined size. A third example, the Haar transform, is characterised by a set of non-periodic, self-similar basis functions of different sizes. The basis functions for an 8x8 image are shown in Fig. 1. The top left image is the basis function associated with the DC value. The three surrounding parent basis functions represent a vertical, diagonal, and horizontal step covering the whole image. All the other basis functions are scaled copies of the larger parent basis functions. Each one represents a local step-like detail of a specific size, position, and orientation. Each point in the original image is covered by exactly one basis function out of each group of equal size and orientation. The Haar transform is complete: any image is exactly represented by its transform coefficients.

Enhancing detail contrast is equivalent to increasing the perceptibility of very subtle image components. According to the MUSICA-approach, detail contrast is enhanced by straightforward manipulation of the transform coefficients. It is implicitly assumed that the basis functions are more or less matched to what we perceive as individual image primitives. This means that each discernible primitive component should be represented by only a few basis functions with non-zero weights. Each basis function then represents a detail of normalised amplitude at a specific scale, and at a specific position in

the image. The shape of the basis functions is not critical within the current context of contrast enhancement. Nevertheless, a set of minimal criteria can be formulated in view of the previous paragraph. First, visual primitives appear locally, hence basis functions need to be *localised* in spatial domain, having non-zero values within a limited extent. Global transforms like FT are inappropriate since their basis functions are poorly localised in spatial domain. Second, primitives of largely varying sizes are present in any image, so basis functions should cover *all scales*. This is not the case with block-oriented transforms like DCT. Third, basis functions with discontinuous behaviour such as the Haar functions are unacceptable because any manipulation of the original coefficients will introduce block-like artefacts in the resulting image. Hence, an appropriate representation calls for a set of *smooth* basis functions with limited spatial extent, which cover the whole image plane, and extend across the entire spatial frequency range (hence the attribute "multiresolution"). Roughly one could think of an image being additively composed of blob-like details of any size, with either positive or negative amplitude.

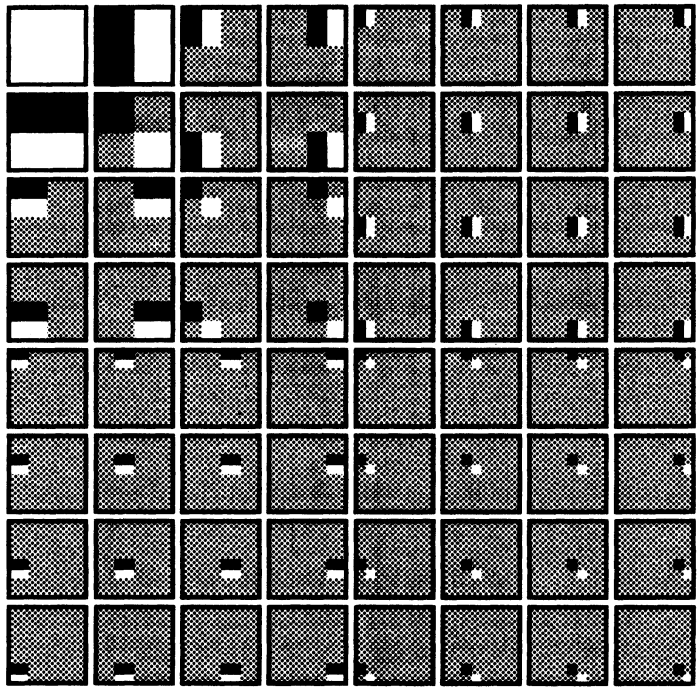

Figure 1: Basis functions of the 2-D Haar transform for an 8x8 image. Grey represents the pixel value 0, black is -1, and white is +1.

Many recent studies on multiresolution representations demonstrate the increasing interest in this research area, mainly directed towards applications of image compression[9,10] and image segmentation[11-12]. A variety of multiscale decomposition schemes meet the above requirements and are suitable for the purpose of detail contrast enhancement. A few categories are briefly described next; the reader is referred to the existing literature for more details.

The Haar transform can be viewed as a special case of the class of (orthogonal) *wavelet* transforms[13]. The wavelet representation can be computed by cascaded application of a two-band splitting quadrature mirror filter (QMF) combination. At each stage the low-pass filter output is decimated by two and fed into the next splitting filter pair. The signal flow is sketched in Fig. 2. The wavelet representation consists of all high-pass responses and the final DC low-pass output. In two dimensions the transform is applied separably, yielding one low-pass, and three high-pass arrays, representing horizontal, vertical, and diagonal detail information at each specific scale. As in the 1-D case only the low-pass components are fed into the next lower resolution stage. The total number of transform coefficients is equal to the original number of samples; this is sufficient for exact reconstruction since the wavelet transform is orthogonal. Adelson et al. worked out nearly-orthogonal QMF implementations with small odd-sized filter kernels for fast computation[14].

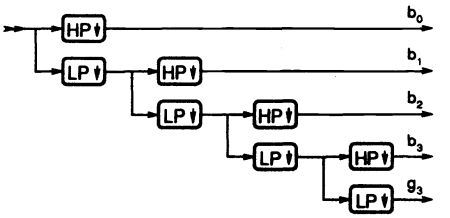

Fig. 2. Cascaded two-band splitting filter bank.

Orthogonality is not a strict requirement within the current context of contrast enhancement. A non-orthogonal transform can still provide exact reconstruction at the expense of some redundancy in the representation. A well-known example is the *Laplacian pyramid* introduced by Burt et al.[15]. This representation consists of a sequence of band-pass images of the original image, each sub-band image covering roughly one octave of the original spatial frequency spectrum. The decomposition and reconstruction processes are schematically drawn in Fig 3.

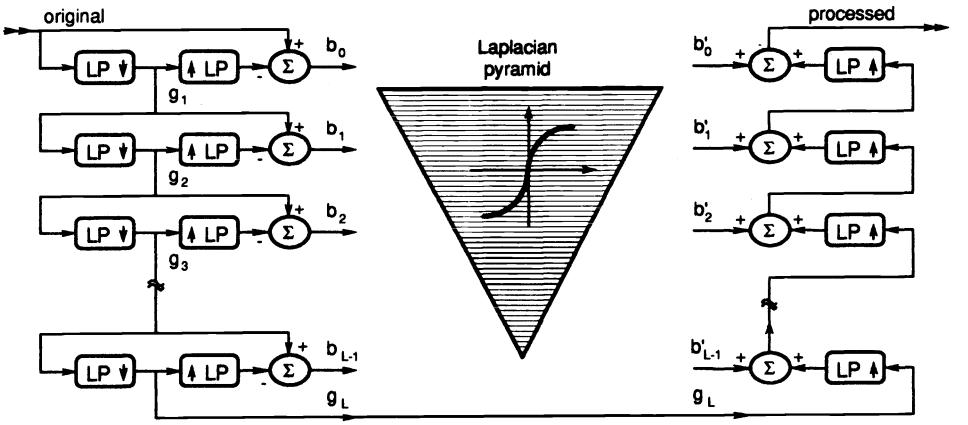

Fig. 3. Flow diagram of the MUSICA-algorithm.

The original image is low-pass filtered and subsampled. This image g_1 is next interpolated to the original array size, and pixelwise subtracted from the original image. This sub-band image b_0 is the finest level of the Laplacian pyramid. The decimated low-pass image g_1 is further low-pass filtered and subsampled yielding g_2; this is interpolated and subtracted from g_1, resulting in the second pyramid layer b_1. All subsequent layers of the Laplacian pyramid b_k are computed by repeating these operations to the subsampled low-pass images g_k from the previous iteration, until the coarsest pyramid image b_{L-1} and the average image value g_L are obtained. The flow of the reconstruction process is drawn at the right hand of Fig. 3. The image average g_L is interpolated to the array size of the next finer pyramid level b_{L-1} and pixelwise added to this. Interpolation and addition are repeated until the reconstructed image at the original resolution level is obtained. The reconstruction is completely reversible if the interpolation filters used in decomposition and reconstruction are identical. Both the low-pass and interpolation filters are applied separately in the horizontal and vertical directions with coefficient values of 0.05, 0.25, 0.4, 0.25, 0.05. With these values the resulting 2-D impulse responses are nearly circularly symmetric, and approach a Gaussian shape after many iterations. This way each Laplacian pyramid plane is in fact the difference of two Gaussian convolutions of different width. The effective width of the subsequent Gaussian kernels increases by a factor of two at each iteration without involving more coefficients; this is because of the decimation. The low-pass filter must provide sufficient bandwidth reduction to avoid aliasing after subsampling. The basis functions associated with the Laplacian pyramid decomposition are overlapping Gaussians of equal size within each pyramid plane. A few basis functions are drawn in Fig. 4. The width doubles at each lower resolution level. The effective shapes near the image border are more complex, and depend on the border extension mechanism used, e.g. constant extension, or reflection. Clearly these basis functions are smooth, are spatially localised, and exist at multiple scales.

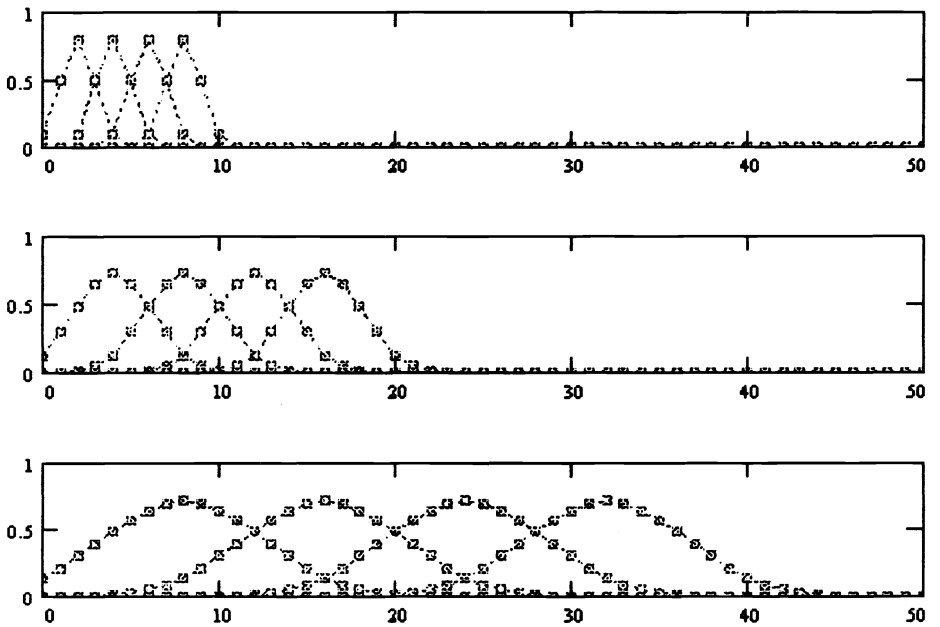

Fig. 4. Basis functions of the Laplacian pyramid transform, for the resolution levels k = 1, 2, 3. Basis functions of level k = 0 (not drawn), are 1-pixel wide impulses, spaced 1 pixel apart. The basis functions near the border will have a more complex shape, depending on the border extension mechanism used.

The actual detail contrast enhancement is achieved by modifying the pyramid coefficients, which is equivalent to altering the amplitude of the corresponding Gaussian image components. Modification is such that small values are amplified, and large values are attenuated, e.g. through non-linear amplification according to the formula:

$$y(x) = aM \frac{x}{|x|}\left(\frac{|x|}{M}\right)^p \tag{1}$$

$$-M < x < M \tag{2}$$

where x represents the original pyramid coefficient $b_{k,i,j}$, and $y(x)$ the modified value $b'_{k,i,j}$, with k the resolution level index, and (i, j) the spatial coordinates. M is the upper bound for coefficient values, and a is a global amplification factor. This factor is needed for constraining the resulting image pixel values to the original dynamic range. The function is monotonic with gradually decreasing slope, in order to attenuate the higher coefficient values. The exponent p controls the degree of non-linearity. A plot of this function is presented in Fig. 5a, for three exponent values: p = 0.6, 0.8, 1.0. The slope at the origin is infinite, causing very small coefficients to be excessively amplified. Unfortunately these coefficients represent homogeneous regions where noise is the dominating image component. In order to limit the amplification of noise to an acceptable level, an alternative conversion function is used:

$$\begin{aligned} y(x) &= aM \frac{x}{x_c}\left(\frac{x_c}{M}\right)^p \qquad \text{if } |x| < x_c \\ y(x) &= aM \frac{x}{|x|}\left(\frac{|x|}{M}\right)^p \qquad \text{if } |x| \geq x_c \end{aligned} \tag{3}$$

$$-M < x < M, \qquad 0 < x_c << M \tag{4}$$

which is a composite function consisting of a linear part around the origin, and a power function defined for the larger abscissas. The cross-over abscissa x_c defines the transition point between the linear function segment and the power function part. By an appropriate selection of the cross-over value as a function of the noise level it is possible to keep the amount of amplification of very subtle details and noise to a reasonable level. The composite function is plotted in Fig. 5b. This non-linear amplification is applied identically to all resolution levels of the pyramid, in order to equalise the amplitude of detail at all scales in the same way.

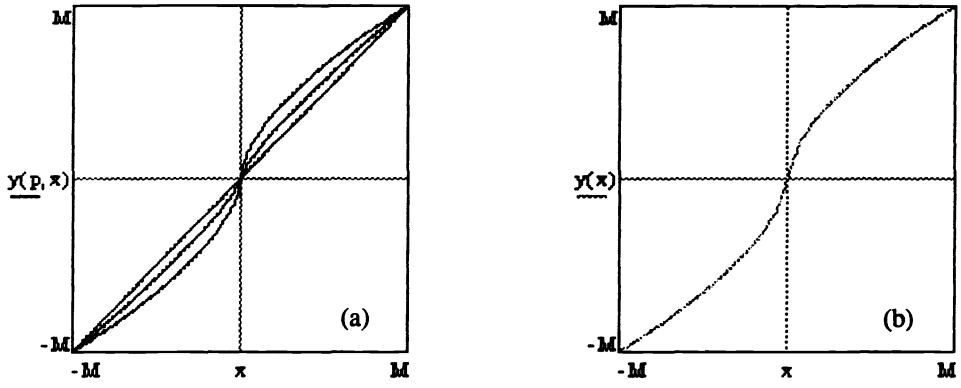

Fig. 5. (a) Power functions for modifying the transform coefficients, exponent values p = 0.6, 0.8, 1.0. (b) composite function for modifying transform coefficients p = 0.6, with linear part around origin for limiting the amount of amplification.

3. RESULTS AND DISCUSSION

The MUSICA-algorithm distinguishes itself from other contrast enhancement methods by the fact that it tends to equalise detail amplitude. Unlike histogram equalisation, which reshapes the image histogram by direct grey value manipulation, the present algorithm applies to *signal variations*, i.e. differential quantities. In its basic form MUSICA has no explicit preference for specific spatial frequencies, in contrast to enhancement techniques based on local neighbourhoods like unsharp masking. However, the current concept requires only a straightforward modification to implement a processing that is equivalent to conventional filtering. A high-pass, low-pass or band-pass filter is created if each pyramid plane is uniformly multiplied by a *scale-specific* weight a_k, where k represents the resolution level of the pyramid plane, instead of applying non-linear amplification with a constant factor a for all pyramid planes as defined in formulas (1) and (3). The particular behaviour of MUSICA in comparison with conventional filtering is demonstrated in Fig. 6, which shows an ankle radiograph. Two different filter types are simulated: a high-pass filter for increasing image sharpness, and a low-suppress filter for reducing the dynamic range by eliminating slowly varying image components. The high-pass filter has a similar effect as unsharp masking with a very small kernel size. The original image is shown in Fig. 6a. Fig. 6c presents the result of MUSICA-processing, with a exponent value of 0.5, i.e. according to a square root characteristic. The (single) weight factor a was adjusted to map the resulting dynamic range back into the original range, so that both images have comparable density ranges. The high-pass filtered image (Fig. 6b) was produced by assigning relative weights of 15 and 3.9 to the pyramid levels k = 0 and k = 1 respectively, i.e. the higher two resolution levels:

$$a_0/15 = a_1/3.9 = a_2 = a_3 = \ldots = a_{L-1} \tag{5}$$

In the low frequency-suppressed image (Fig. 6d) the lower resolution pyramid planes were assigned smaller weights:

$$a_0 = 1.6a_1 = 2.7a_2 = 4.3a_3 = 7.1a_4 = 11.5a_5 = 19a_6 = 31a_7 = 50a_{L-1} \tag{6}$$

In the latter two cases the amplification was uniform across each pyramid plane to simulate the pure effect of conventional filtering. The actual values of the weight factors a_k were also adjusted to obtain similar density ranges as the original image. The signal profile of the middle image line is plotted on top of each image. The profile of the original image

exhibits a gradual increase from left to right, with a steep falling edge at the right border of the irradiation field. Detail contrast is very low due to the wide exposure latitude. The MUSICA-enhanced image displays all the existent image structure both in soft tissue and bony regions, without stressing high contrast edges. Larger-scale features which were invisible in the original image, are clearly discernible, like the dark zone in the centre of the image. High-frequency emphasis on the other hand (Fig. 6b) only stresses the fine-scale details and does not significantly improve the overall contrast. The emphasis of noise in a narrow frequency band yields the fine-grain texture typical for this kind of processing. Overshoots at step edges are clearly visible too, e.g. at bone-soft tissue interfaces, and at the irradiation field border. This kind of artefact does not appear in the MUSICA-processed image (Fig. 6c). Suppression of the lower spatial frequencies in Fig. 6d enhances contrast, but not in such a uniform way as with MUSICA: the brighter image regions mainly in the left-central part of the image still have very poor contrast. An additional drawback is the risk of density gradient reversal in cases like this where the suppression factor is large; a phenomenon which shows up in the rightmost bone region.

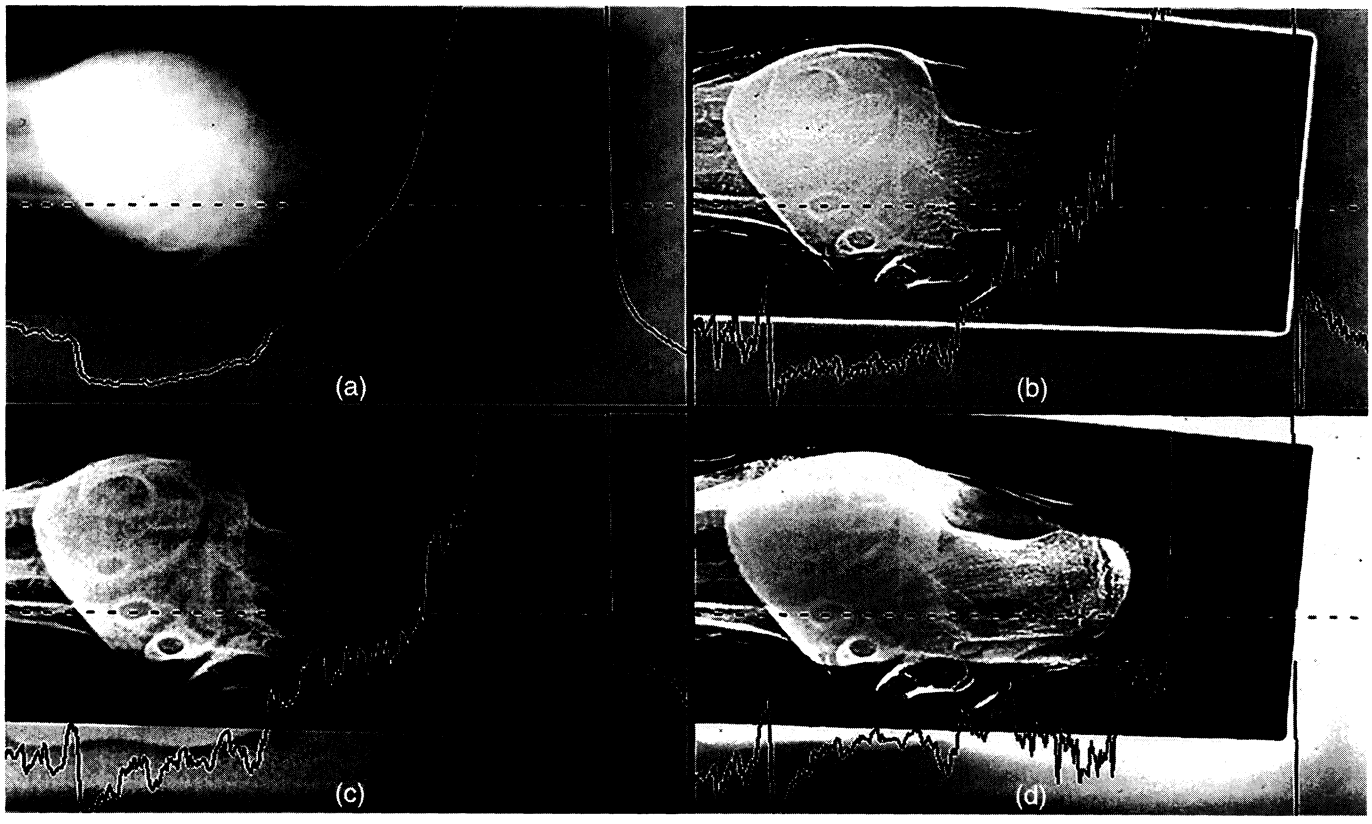

Fig. 6. (a) original image; (b) high-frequency emphasis; (c) MUSICA-enhancement; (d) low-frequency suppression

The above considerations are clarified in Figs. 7-10, which show each of the previous images together with their Laplacian pyramid planes. Only even resolution levels are shown, starting from the highest level. All pyramid images have zero mean, which is displayed as medium grey. The equalising effect of MUSICA with respect to detail amplitude is apparent from the comparison of Figs. 7 and 8. In the high-emphasised image (Fig. 9), only the topmost Laplacian pyramid image is different from the original pyramid images. Very large signal peaks at high contrast edges are caused by uniform amplification across the image plane. The low-suppressed image shown in Fig. 10 looks different from the original in all of its pyramid planes, although only the lower resolution levels are suppressed. This is caused by adjusting the overall amplification to match the original density range. The global brightness decrease from left to right, clearly visible in the lower resolution pyramid plane of the original image, is apparently reduced in the low-suppressed image (Fig. 10e). The problem of density gradient reversal appears in those regions (e.g. the rightmost ankle part) which originally have a strong

positive gradient in the lower resolution levels, which is strongly suppressed (Fig. 10e); and a negative gradient in the higher levels, which is less suppressed (Figs. 10c,d), or vice versa.

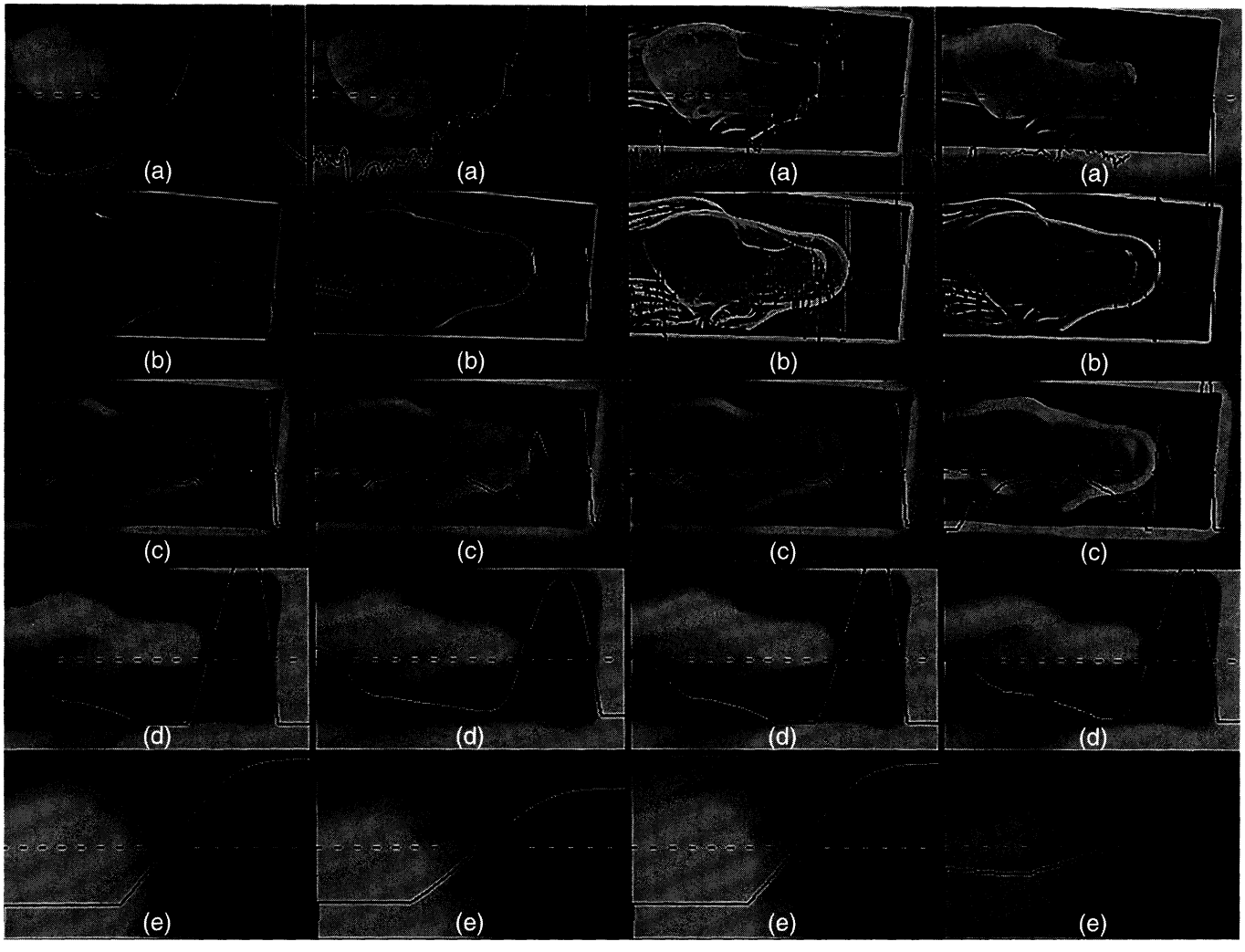

Figs. 7-10. From left to right: original image, MUSICA-enhanced, high-emphasised, low-suppressed. (a) reconstructed images; (b)-(e) Laplacian pyramid image planes at resolution levels 0, 2, 4, and 6, resp.

The previous pictures showed examples of high-emphasis, low-suppression, and MUSICA-processing, all applied to an exaggerated degree for the purpose of comparison. Careful usage of some additional filtering can be beneficial, however, as is demonstrated in the picture of Fig. 11b, which was processed with a power value of 0.75, and additional high-emphasis (factor 2 for highest resolution plane), and low-suppression (factor 1/3 for the lowest resolution).

The effect of varying the non-linearity of detail amplification by means of the power function exponent is illustrated in Fig. 12a-d, with values p = 1, 0.85, 0.7, and 0.5 respectively, applied to a lateral chest examination. The optimal value depends upon the viewing medium; for film diagnosis this is between 0.7 and 0.8, for nearly all examination types. These values came out of extensive comparative studies at the university hospitals, U.Z. Gasthuisberg, Leuven, Belgium, and Georgetown University Hospital, Washington D.C, and were confirmed in routine at the Frauen Und Kopfklinik, Innsbruck, Austria. The algorithm requires no further parameter tuning.

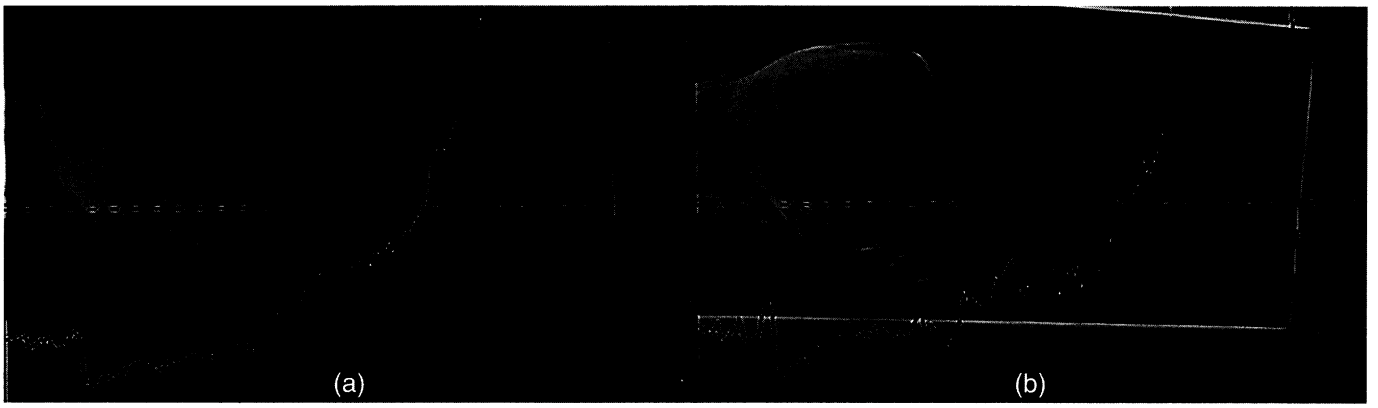

Fig. 11. (a) MUSICA-enhanced image; (b) combination of MUSICA-enhancement, high-frequency emphasis, and low-frequency suppression.

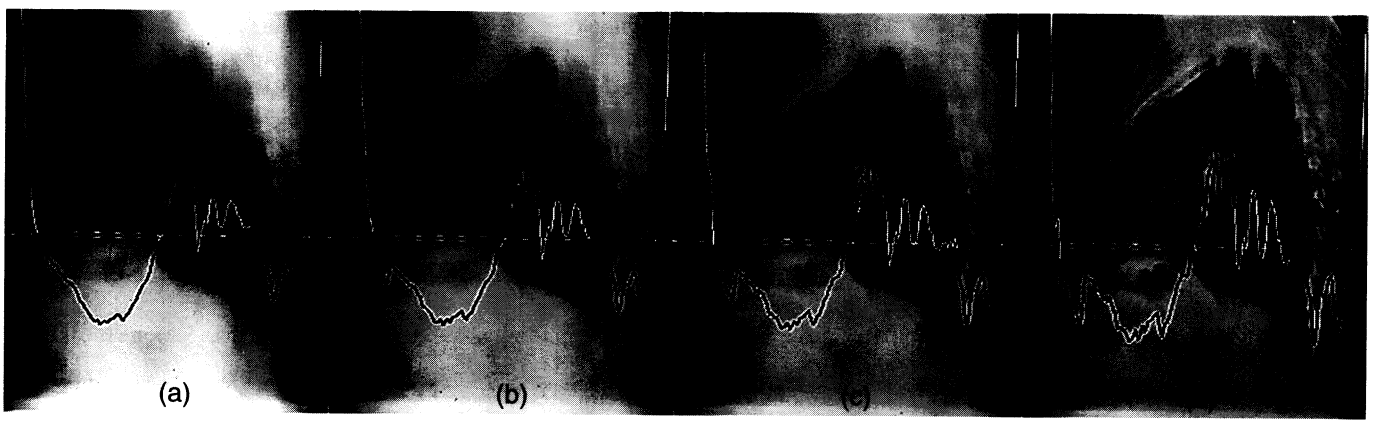

Fig. 12. (a) original image; (b)-(d) various degrees of MUSICA-enhancement, p = 0.85, 0.7, and 0.5 resp.

4. CONCLUSIONS

We have presented a novel algorithm for enhancement of detail contrast in computed radiography images with excellent performance, and without introducing artefacts. The concept has a general scope, and can be used for other medical modalities, such as computed tomography or digital mammography, or in non-medical application areas, such as non-destructive testing, prepress, or photofinishing. The method is based on simple manipulation of coefficients of a suitable multiresolution representation, such as a wavelet decomposition, or the Laplacian pyramid. The actual enhancement operation requires very little computation power if it is implemented by means of a lookup table, and it can be elegantly combined with additional filtering such as high-emphasis or background suppression. The decomposition and reconstruction processes are the most time-consuming parts of the algorithm. However, very efficient computation schemes exist such as the Burt pyramid based on cascaded application of small kernel, separable convolutions.

The MUSICA-algorithm has been routinely applied to tens of thousands of CR images, for the following examinations: chest, skull, spine, shoulder, pelvis, extremities, and abdomen, with excellent acceptance. No artefacts have ever been perceived at very high contrast edges. The images look quite natural, presumably because the involved operations are smooth, and are uniformly applied to all scales. Unlike most enhancement methods based on sliding neighbourhoods, the algorithm needs no stringent examination-specific parameter tuning. Moreover, the extraction of the diagnostic signal range for optimal viewing becomes less critical when the images are enhanced by the MUSICA-algorithm. This is an important

benefit since the automatic selection of the optimal signal range for each individual examination is often critical, e.g. in field-limited or wide-latitude exposures.

The contents of this article form subject matter of several patent applications.

5. ACKNOWLEDGEMENTS

This research project is supported by the "Flemish Institute for the Promotion of Scientific and Technological Research in the Industry", I.W.T.

6. REFERENCES

1. S. M. Pizer, E. P. Amburn, J. D. Austin, R. Cromartie, A. Geselowitz, T. Greer, B. Ter Haar Romeny, J. B. Zimmerman, and K. Zuiderveld, "Adaptive histogram equalisation and its variations", *Computer Vision, Graphics, and Image Processing*, Vol. 39, pp. 355-368, 1987.

2. M. L. Cocklin, A. R. Gourlay, P. H. Jackson, G. Kaye, I. H. Kerr, and P. Lams, "Digital processing of chest radiographs", *Image and Vision Computing*, Vol. 1, No. 2, pp. 67-78, 1983.

3. M. Prokop, C. Schaefer, J. W. Oestmann, A. Meschede, S. Reichelt, and M. Galanski, "Optimal parameters for unsharp mask filtering in digital chest radiographs", *Proc. Intern. Symposium CAR '91*, pp. 149-154, Springer Verlag, 1991.

4. M. Prokop, M. Galanski, J. W. Oestmann, U. von Falkenhausen, H. Rosenthal, P. Reimer, J. Nischelsky, and S. Reichelt, "Storage phosphor versus screen-film radiography: effect of varying exposure parameters and unsharp mask filtering on the detectability of cortical bone defects", *Radiology*, Vol. 177, No. 1, pp. 109-113, Oct. 1990.

5. J. W. Oestmann, M. Prokop, C. M. Schaefer, and M. Galanski, "Artefacts in digital storage phospor radiography", *Proc. Intern. Symposium CAR '91*, pp. 122-126, Springer Verlag, 1991.

6. U. Bick, W. Wiesmann, H. Lenzen, M. Fiebich, H.-J. von Lengerke, and P. E. Peters, "Utilizing digital luminescence radiography in pediatric radiology: a report of initial experiences", *Electromedica*, Vol. 59, No. 1, pp. 26-30, 1991.

7. K. Rehm and W. J. Dallas, "Artifact suppression in digital chest radiographs enhanced with adaptive histogram equalisation", *Proc. SPIE*, Vol. 1092, pp. 290-300, 1989.

8. M. I. Sezan, A. M. Tekalp, and R. Schaetzing, "Automatic anatomically selective image enhancement in digital chest radiography", *IEEE Trans. on Medical Imaging*, Vol. 8, No. 2, pp. 154-162, June 1989.

9. J. H. Arbeiter, "Multidimensional video image processing architecture", *Optical Engineering*, Vol. 25, No. 7, pp. 875-880, July 1986

10. H. Gharavi and A. Tabatabai, "Sub-band coding of digital images using two-dimensional quadrature mirror filtering", *Proc. SPIE*, Vol. 707, pp. 51-61, 1986.

11. M. Unser, and M. Eden, "Multiresolution feature extraction and selection for image segmentation", *IEEE Trans. on Pattern Analysis and Machine Intelligence*, Vol. 11, No. 7, pp. 717-728, July 1989.

12. L. M. Lifshitz, and S. M. Pizer, "A multiresolution hierarchical approach to image segmentation based on intensity extrema", *IEEE Trans. on Pattern Analysis and Machine Intelligence*, Vol. 12, No. 6, pp. 529-540, June 1990.

13. S. G. Mallat, "A theory for multiresolution signal decomposition: the wavelet representation", *IEEE Trans. on Pattern Analysis and Machine Intelligence*, Vol. 11, No. 7, pp. 674-693, July 1989.

14. E. H. Adelson, E. Simoncelli, and R. Hingorani, "Orthogonal pyramid transforms for image coding", *Proc. SPIE*, Vol. 845, pp. 50-58, 1987.

15. P. J. Burt, and E. H. Adelson, "The Laplacian pyramid as a compact image code", *IEEE Trans. on Communications*, Vol. 31, No. 4, pp. 532-540, 1983.